

HOSTED BY



ELSEVIER

Contents lists available at ScienceDirect

Egyptian Journal of Ear, Nose, Throat and Allied Sciences

journal homepage: www.ejentas.com

Original article

Computed tomography anatomy of the paranasal sinuses and anatomical variants of clinical relevants in Nigerian adults ☆

Regina Chinwe Onwuchekwa ^{a,*}, Nengi Alazigha ^b^a Department of Radiology, Faculty of Clinical Sciences, College of Health Sciences, University of Port Harcourt, Nigeria^b Department of Radiology, Braithwaite Memorial Specialist Hospital (BMSH), Port Harcourt, Nigeria

ARTICLE INFO

Article history:

Received 8 August 2016

Accepted 12 November 2016

Available online xxxx

Keywords:

Paranasal sinuses

Computed tomography

Nasal turbinate

Ostiomeatal complex

Radiologic anatomy

ABSTRACT

Aim: The aim of the study is to show the anatomy of the paranasal sinuses as delineated by the computed tomography and to describe the variants which not only predispose to chronic sinusitis but may lead to complications in endoscopic sinonasal surgery.

Introduction: The paranasal sinuses are group of air filled spaces surrounding the nasal cavity. Paranasal sinuses start developing from the primitive choana at 25–28 weeks of gestation. Three projections arise from the lateral wall of the nose and serve as the beginning of the development of the paranasal sinuses.

Materials and methods: This was a prospective study carried out in a tertiary institution. 110 patients without paranasal sinus symptoms who presented for head computed tomography studies and gave consent for a coronal section scan of the paranasal sinuses to be taken in addition to the axial section of the head were included in the study. The CT examination was performed with GE Hispeed-NX/I Base-2002 Dual Slice Helical Computed tomography machine.

Results: There were 48 females and 62 males giving a male female ratio of 1:1.3. Among these 229 cases of anatomical variants were observed. The commonest anatomical variants were pneumatization of the middle nasal turbinates (32.73%). This is followed by agger nasi cells 23.64%, Haller's cells 20.91%, septal deviation 20.18% and sphenoid sinus septation (18%).

Conclusion: Computed tomography is the gold standard in the radiologic investigation of the paranasal sinuses, either for diagnosis for sinonasal lesions or pre and post-surgical assessment. Its capability in delineating the anatomical variants in paranasal sinuses protects against iatrogenic injury to essential structures around the paranasal sinuses and recurrent diseases from extramural cells.

© 2016 Egyptian Society of Ear, Nose, Throat and Allied Sciences. Production and hosting by Elsevier B.V. This is an open access article under the CC BY-NC-ND license (<http://creativecommons.org/licenses/by-nc-nd/4.0/>).

1. Introduction

The paranasal sinuses are group of air filled spaces surrounding the nasal cavity; which start developing from the primitive choana at 25–28 weeks of gestation.¹ Three projections arise from the lateral wall of the nose and serve as the beginning of the development of the paranasal sinuses. The anterior projection forms the Agger nasi, the inferior or maxilloturbinate projection forms the inferior turbinates and maxillary sinus, while the superior or ethmoidoturbinate projection forms the ethmoidal air cells and their corresponding drainage channels. The sinuses are named from the facial

bones in which they are located. The maxillary and ethmoid sinuses are aerated at birth, while the sphenoid sinuses and frontal sinuses are pneumatized at about the 2nd and 6th year of life respectively.¹ The sinuses reach the adult size at adolescent age.¹

Radiologic evaluation of the paranasal sinuses is essential in delineating the location and extent of sinonasal diseases and in planning surgical intervention. Plain radiography, computed tomography and magnetic resonance imaging are applied in evaluating the sinuses.

Standard paranasal sinus radiograph can readily demonstrate the maxillary or frontal sinus diseases but incompletely delineates ethmoid sinus due to overlapping of structures.² The role of Magnetic resonance imaging is limited but may provide information on paranasal sinuses fungal infection and differentiating thickened mucosa from fluid retention.

Computed tomography is considered the method of choice in delineating completely the normal anatomy and anatomical

Peer review under responsibility of Egyptian Society of Ear, Nose, Throat and Allied Sciences.

* Corresponding author at: Department of Radiology, Faculty of Clinical Science, College of Health Sciences, University of Port Harcourt, Rivers State, Nigeria.

E-mail address: chichewas2003@yahoo.com (R.C. Onwuchekwa).

<http://dx.doi.org/10.1016/j.ejenta.2016.11.001>

2090-0740/© 2016 Egyptian Society of Ear, Nose, Throat and Allied Sciences. Production and hosting by Elsevier B.V.

This is an open access article under the CC BY-NC-ND license (<http://creativecommons.org/licenses/by-nc-nd/4.0/>).

Please cite this article in press as: Onwuchekwa R.C., Alazigha N. Computed tomography anatomy of the paranasal sinuses and anatomical variants of clinical relevants in Nigerian adults. Egypt J Ear Nose Throat Allied Sci (2016), <http://dx.doi.org/10.1016/j.ejenta.2016.11.001>

variants of the paranasal sinuses and it is extremely useful in the pre-operative planning and in post operative follow-up in cases of endonasal interventions.

The development of the paranasal sinuses especially the ethmoid labyrinth is associated with anatomical variations.³ Some of which are common while others are rare. Recognition of these variants is important to both the rhinologist and radiologist. Proximity of these occasional cells to the main drainage pathway of the paranasal sinuses may reduce the mucociliary clearance, thus predisposing to inflammatory processes and causing endonasal endoscopic surgery complications.

The aim of this study is to show the anatomy of the paranasal sinuses as delineated by the computed tomography among Nigerian adults and to describe the variants which not only predispose to chronic sinusitis but may lead to complications in endoscopic sinonasal surgery.

2. Materials and methods

We retrospectively searched our radiology database for all cases of computed tomography scan of the paranasal sinuses obtained in the Radiology department of our health institution over a three year period (March 2011 to February 2014). The patients were referred for computed tomography (CT) scan due to a clinical symptoms referable to sinonasal region. A total of 365 consecutive CT studies of the paranasal sinuses were identified; Patients with facial trauma, positive paranasal sinus pathology, head and neck tumours and previous surgery were excluded. Of the 365 CT studies, 255 were excluded leaving a total of 110 participants, made up of 62 males and 48 females with age range between 18 years and 82 years. The CT examination was performed with GE Hispeed-NX/I Base-2002 Dual Slice Helical Computed tomography machine. The coronal section slice thickness was 5 mm with table index of 4 mm. The section was taken from anterior frontal sinus to posterior sphenoid sinus. KVP was 125, mAs was 450 and scan time was 5 sec. Each patient was positioned prone with the head hyperextended on the scanner couch. The gantry angulation was perpendicular to the infraorbitomeatal line (IOML). The axial slice thickness was 3 mm taken every 3 mm intervals. The patient was placed in supine position. Gantry angulation was at IOML and the section was taken from hard palate to the roof of the frontal sinus. The exposure factors were same as in the coronal scan. The images were analysed by the authors who are radiologist with more than ten years of experience.

Our institutional ethical committee approved the study.

Detailed analysis of the anatomy of the structures visualized were made, and significant anatomical variants were noted. Sagittal reconstructions were also done for detailed assessment of the structures.

2.1. Anatomy of the paranasal sinuses, osteomeatal complex and nasal walls

Maxillary sinuses (Fig. 1): the maxillary sinus is pyramidal in shape with the apex in the zygomatic process of the maxilla bone and the base at the lateral wall of the nose. Behind the posterior wall are the infratemporal and pterygopalatine fossae. The roof of the sinus is the floor of the orbit. The floor of the sinus is the alveolar part of the maxilla. The adult sinus varies in size. Some are large and extend into the zygomatic process of the maxilla and into the alveolar process so that the roots of the molar and premolar teeth lie immediately beneath the floor or project into it.

The maxillary sinus drains via its ostium which opens at the posterior part of the infundibulum and empties into the middle meatus in the lateral wall of the nose (Fig. 1). Occasionally, there

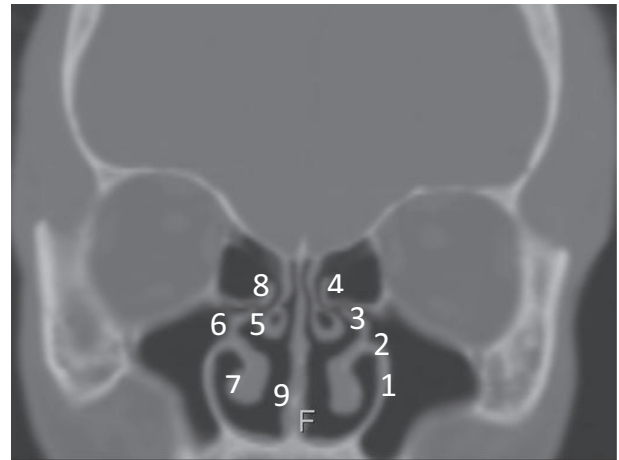


Fig. 1. A coronal CT image demonstrating the osteomeatal complex and the nasal cavity. (1) Maxillary sinus, (2) maxillary ostium, (3) infundibulum, (4) ethmoidal bulla, (5) middle nasal turbinate, (6) uncinate process, (7) inferior nasal turbinate, (8) hiatus semilunaris, (9) nasal septum.

is an accessory ostium which opens anterior or posterior to the lower part of the uncinate process of the inferior turbinate.

Ethmoid sinuses: The ethmoid bone is a delicate complex structure which consists of four parts: a horizontal lamina called the cribriform plate, a perpendicular plate, and two lateral masses called the labyrinths (Fig. 3). The lateral wall of the labyrinth forms the medial wall of the orbit and this is called lamina papyracea; it is a paper thin bone. Each ethmoidal labyrinth consists of multiple thin walled, highly variable air cells arranged in three groups;

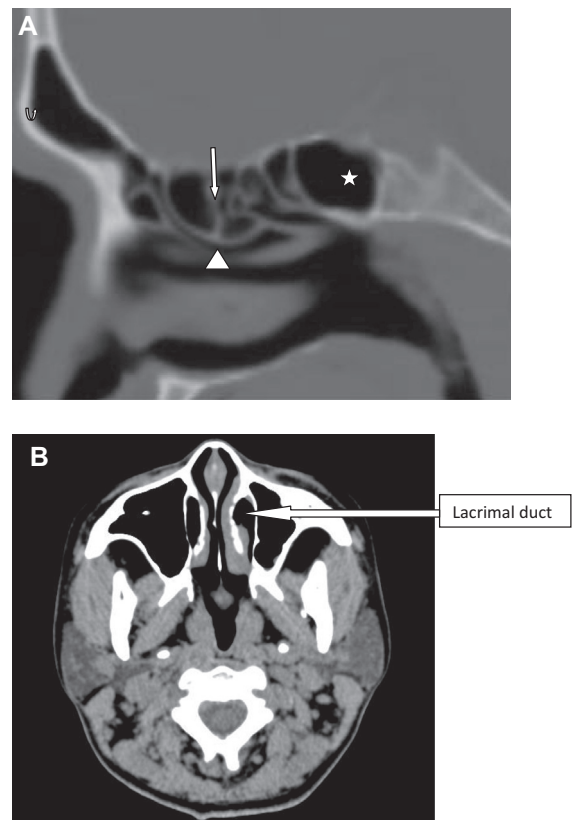


Fig. 2. (A) Sagittal CT image of the paranasal sinus shows frontal sinus (curved up arrow), frontal recess (arrow head), ethmoidal sinus (arrow) and sphenoidal sinus (star).

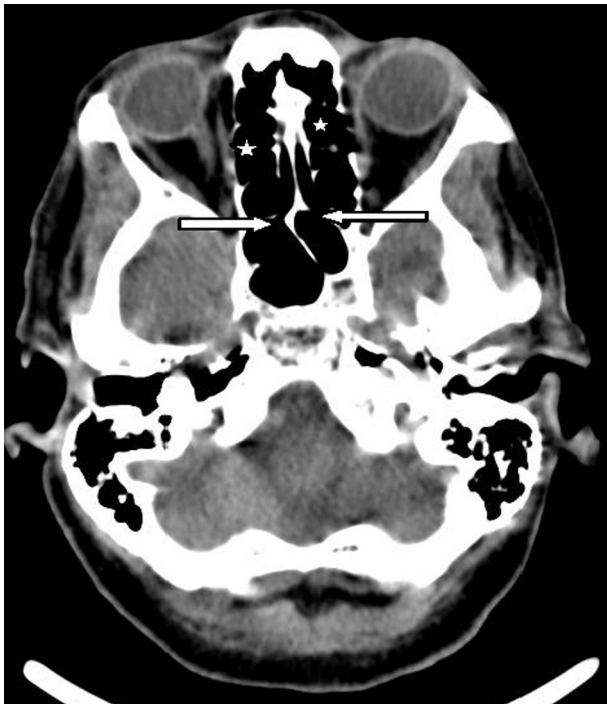


Fig. 3. Axial CT image shows the sphenoid sinuses and the sphenoethmoidal recess (arrows), Ethmoidal labyrinths (star).

anterior, middle and posterior clusters. The anterior and middle ethmoid cells open only at their aperture or ostia which drains via the infundibulum into the middle meatus at the lateral wall of the nasal cavity. At the back of the labyrinth the wall of the posterior ethmoidal air cells is completed by fusion of the orbital process of the palatine bone and the sphenoid bone. The ostia of the posterior air cells open into the superior meatus. The superior and middle nasal conchae project from the medial wall of the ethmoid sinus.

Sphenoid sinuses: Two sphenoid sinuses occupy the sphenoid bone. The septum is a thin bone which is hardly in the center. The posterior aspect of the sphenoid sinuses may be septated. Sphenoid sinus is known as being the most variable cavity of the human body, which makes it difficult to approach and assess the sinuses.⁴ The sinus is surrounded by vital structures such as the internal carotid artery (ICA), optic nerve (ON), and vidian canal (VC). The size of the sinuses varies depending on the extent of pneumatization. The ostium is in the anterior wall and this is better demonstrated in the axial CT images. Each ostium opens into the sphenoethmoidal recess behind the superior concha which is a common drainage for the sphenoid sinus and the posterior ethmoid cells (Fig. 3).

Frontal sinus: It lies in the diploe space between the outer and inner tables of the frontal bone. The two sinuses are commonly unequal in size and extent and are separated by a bony septum in the midline. Occasionally, one is very small in size or may be absent. The sinus drain via frontal recess (Fig. 2) which is an hourglass shaped structure and usually drains into the middle meatus in 62% or into the ethmoid infundibulum in 38%.⁵

Ostiomeatal complex or unit: this comprises of the maxillary sinus ostium, the ethmoidal infundibulum, anterior ethmoid cells and the frontal recess. It is the anterior drainage pathway of the sinuses. The maxillary sinus ostium and the infundibulum serve as the predominant channel linking the maxillary sinus with the nasal cavity. The infundibulum is bounded laterally by the infero-

medial wall of the orbit. Superiorly by the hiatus semilunaris and ethmoid bulla, medially by the uncinate process and inferiorly by the maxillary sinus as the sinus funnels into it (Fig. 1). The infundibulum represents the superomedial extension of the maxillary ostium.

Turbinates: Usually there are three nasal turbinates in each nasal cavity. These are the superior, middle and the inferior turbinates. Sometime there may be a 4th one called supreme turbinate which is located lateral to the superior turbinate. The middle turbinate is a thin scroll sheet of bone formed from the medial portion of the ethmoid bone. It lies inferomedial to the anterior ethmoid air cells and attached vertically to the cribriform plate superiorly and to the lamina papyracea laterally via a bony strut, the basal lamella. The basal Lamella divides the ethmoidal cells into the anterior and posterior ethmoidal cells. The middle turbinate continues posteriorly in an axial plane, forming the roof for the posterior portion of the middle meatus. This three dimensional orientation gives the middle turbinate exceptional stability. Beneath each turbinate is a meatus. The anterior ethmoidal cells drain into the middle meatus, the posterior ethmoidal cells drain into the superior meatus while the lacrimal duct drains into the inferior meatus.

Ethmoidal bulla (Fig. 5): The ethmoidal bulla is the largest and most constant of the anterior ethmoid cells, however its degree of pneumatization varies considerably, ranging from failure of pneumatization (torus ethmoidalis) to a giant ethmoid bulla. It is an intramural ethmoid cell which is in intimate relationship with the ostiomeatal unit. It is bordered inferomedially by the infundibulum and hiatus semilunaris, laterally by the lamina papyracea and superoposteriorly by the sinus lateralis. It drains into the middle meatus through a pneumatized retrobulbar tract.

Crista galli: The crista galli is in the midline above the cribriform plate. The falx cerebri attaches to its thin and slightly curved posterior border, whereas its shorter thicker anterior border is joined to the frontal bone by two small alae, completing the margins of the foramen caecum. Embryologically, the crista galli is derived from the ethmoid bone.¹

Uncinate process: on CT, the uncinate process is a wing or boomerang shaped piece of bone. It is attached inferiorly to the inferior turbinate. Anteriorly the uncinated process is attached to the nasolacrimal apparatus; posteriorly it has a free margin; and superiorly its attachment is variable. It may attach to the skull base, the middle turbinate or lamina papyracea. This variable attachment has its clinical implications.

Nasal septum (Fig. 1): the nasal septum constitute the medial wall of the nasal cavity. It lies between the roof and floor of the nasal cavity, thus it extends from the cribriform plate superiorly to the hard palate inferiorly. It is formed by the septal cartilage anteriorly and the vomer and perpendicular plate of the ethmoid bone posteriorly. The structures that make up the nasal septum are aligned to form a straight wall.

Lacrimal duct (Fig. 2B). The lacrimal bone articulates with the nasal bone and with the inferior concha, enclosing between them the canal for the nasolacrimal duct which opens into the upper part of the inferior meatus about 1 cm behind the anterior end of the concha.

3. Result

Of the 110 participants included in the study, there were 229 anatomical variants recorded (Table 1). The commonest anatomical variants were pneumatization of the middle nasal turbinates 32.73%, agger nasi cells 23.64%, Haller's cells 20.91%, septal deviation 20.18% and sphenoid sinus septation (18%).

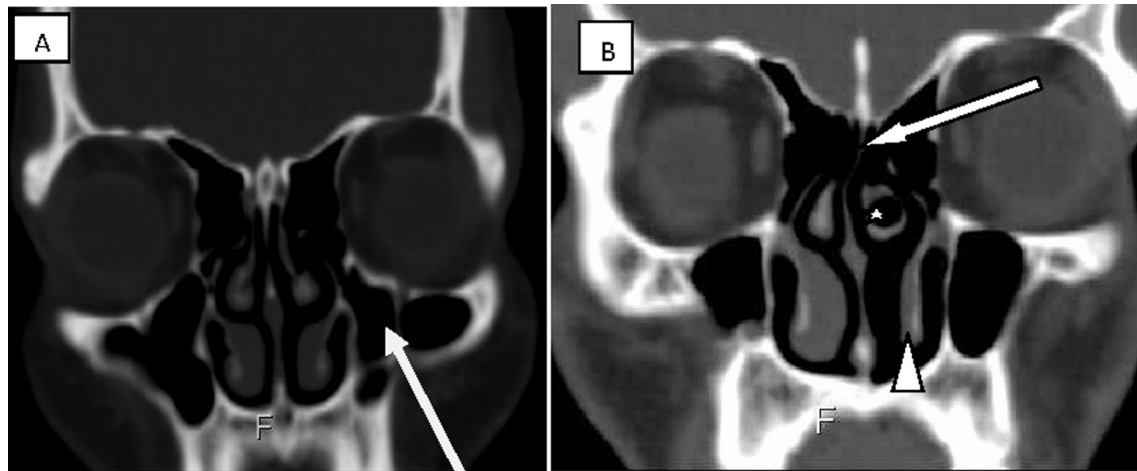


Fig. 4. Coronal CT images showing (A) multiple septations in the left maxillary sinus (arrow), (B) pneumatized left middle conchae (white star), hypoplastic left inferior conchae (arrow head), deviated nasal septum (long arrow).

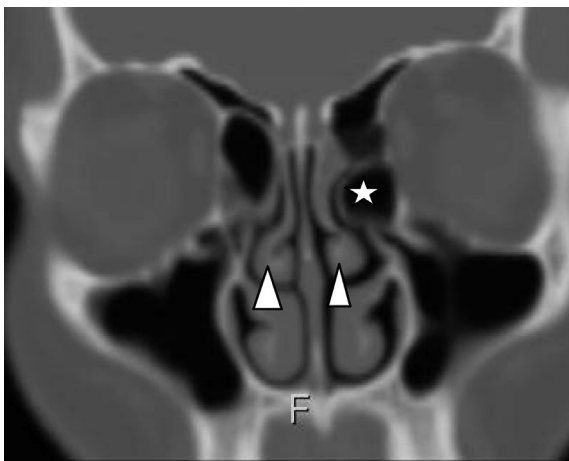


Fig. 5. Coronal CT image shows bilateral paradoxical middle turbinate (arrow head) and ethmoid bulla (star).

4. Discussion

4.1. Maxillary sinus variants

Asymmetry in the size and shape of the maxillary sinus is common. There may be Extension of pneumatization of the maxillary sinus towards the palatine recess and alveolar recess. There could also be septations of the maxillary sinuses (Fig. 4A). Occasionally accessory ostium may be present which are generally solitary, but may be multiple. Accessory maxillary ostium may be congenital or secondary to sinonasal diseases.⁶

4.2. Nasal turbinates variants

Pneumatization of the conchae is one of the most common variations of sinonasal anatomy. Middle turbinate is the most frequent site of pneumatization whereas the superior turbinate and the inferior turbinates are less frequent sites. The pneumatization of the middle turbinate (Figs. 4B and 6) may involve the vertical lamella, bulbous segment or both. Depending on the degree of middle turbinate pneumatization, it may be associated with middle meatus or infundibulum obstruction. The prevalence of middle turbinate pneumatization in this study was 32.73% which is within

Table 1

The bony anatomical variations and the frequency.

| Variants | Number of patients (%) |
|---|------------------------|
| <i>Frontal sinus</i> | |
| Extended | 1(0.91%) |
| Hypoplastic | 4(3.64%) |
| <i>Maxillary sinuses</i> | |
| Septation | 7(6.36) |
| Hypoplasia | 1(0.91) |
| Extended | 3(2.73) |
| <i>Sphenoid sinus</i> | |
| Septation | 20(18.18) |
| Extensions | 12(10.91) |
| Anterior clinoid pneumatization | 7(6.36) |
| Ondi cells | 8(7.27) |
| <i>Ethmoid sinus</i> | |
| Supra orbital cells | 7(6.36) |
| Frontal cells | 14(12.73) |
| Agger nasi | 26(23.64) |
| Haller's cells | 23(20.91) |
| <i>Turbinates</i> | |
| Superior turbinate pneumatization | 7(6.36) |
| Agnesis of both nasal turbinates | 1(0.91) |
| Middle turbinate pneumatization | 36(32.73) |
| Inferior turbinate pneumatization | 1(0.91) |
| Hypoplastic inferior turbinate | 16(14.55) |
| Paradoxical middle turbinate | 2(1.82) |
| Fusion of septum and inferior turbinate | 1(0.91) |
| <i>Nasal septum</i> | |
| Deviation of nasal septum | 23(20.91) |
| Crista galli/septal pneumatization | 9(8.18) |

the range reported by other authors. Asruddin et al.⁷ Mamitha et al.⁸ Zinreich et al.² and Weinberger et al.⁹ reported prevalence of 30%, 28%, 16% and 15% respectively. Higher prevalence was reported by Aramani et al.¹⁰ Perez-Pinas et al.¹¹ and Scribano et al.¹² who got 53.7%, 73% and 67% respectively.

There may also be abnormal curvature of the middle turbinate towards the midline and this is called the paradoxical middle turbinates (Fig. 5). There may also be an accessory or secondary middle turbinate but non was found in this study. Depending on the degree of the curvature of the paradoxical turbinate, compression of the infundibulum and obstruction may be observed.

The anatomical variation of the inferior turbinates are rare. Pneumatization of the inferior turbinate, bifid inferior turbinates and hypertrophy or hypoplasia (Fig. 4B) of the osseous and soft

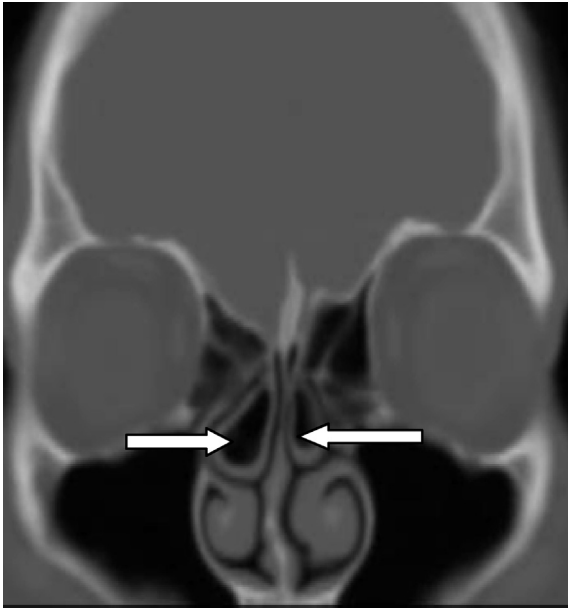


Fig. 6. Coronal CT image shows bilateral middle turbinate pneumatization (arrow).

tissue of the inferior turbinates are some of the reported alterations of this structure.

4.3. Sphenoid sinus variants

Sphenoid sinuses have variable pneumatization extent. There may be extension of pneumatization of the sphenoid sinus towards the lateral recess of the sphenoid bone (bilateral), the clinoid pro-

cess (Fig. 7B), the vomer, palatine bone, the lesser wings, greater wings, the pterygoid process (Fig. 7C) and clivus. Pneumatization of the anterior clinoid process may be unilateral or bilateral; anterior clinoid pneumatization was noted in 7 (6.36%) patients in this study. This is similar to 13% recorded by Bolger et al.¹³ in a study of 202 patients and 4% recorded by Delano et al.¹⁴ in 300 patients who underwent CT scan of the paranasal sinuses.

There may be dehiscence in the bony wall between the carotid arteries and the sphenoid. Deviation of the septum or multiple septa (Fig. 7D) may be present.

With extensive pneumatization, the bone covering the carotid arteries, optic nerves, maxillary nerves and vidian nerve can be thin or even absent, making these structures susceptible to iatrogenic injuries.¹⁵

4.4. Frontal sinus variants

The frontal sinus varies in its extent of pneumatization, there may be increased sinus aeration beyond the normal margin of the sinus. The lamina of the frontal bone and the crista galli may also be pneumatized. The crista galli cells mostly originate from the frontal sinus, although in some cases it may be the result of spread of the anterior ethmoidal cells. In our series, pneumatized crista galli (Fig. 10D) was found in 9 (8.18%) cases. This prevalence is in keeping with finding by Basic et al.¹⁶ using CT scans in a series of 212 patients noted pneumatization of the crista galli in 2.4%. Also Som et al.¹⁷ found pneumatized crista galli in five patients (2.4%).

Hypoplasia of the frontal sinus was found in 3.64% of the participants and extensive pneumatization in 0.91%. Hypoplastic frontal sinus was detected in 10.6% of patients in a study in Iran¹⁸ and in 8.4% of patients in the study by Stallman in Germany.¹⁹

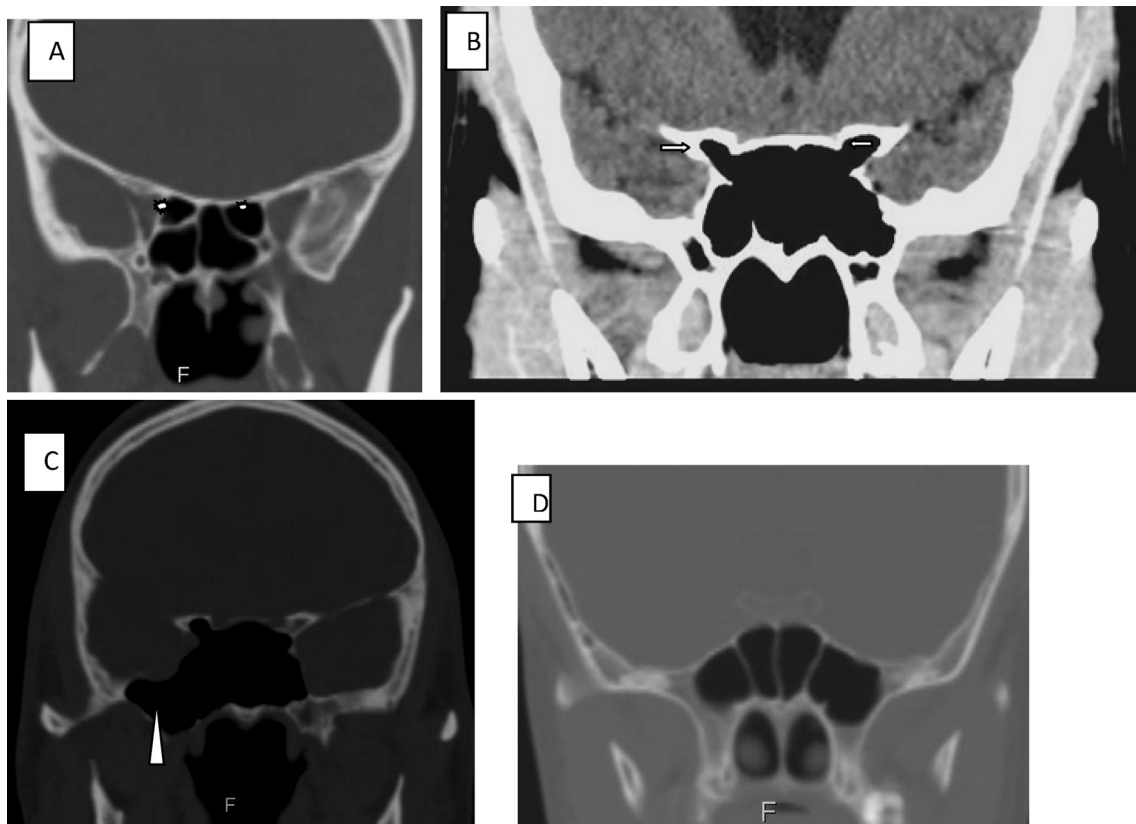


Fig. 7. Coronal CT images shows (A) Onodi cells (explosion), (B) extension into the anterior clinoid process bilaterally (arrows), (C) extension into the right pterygoid plate (arrow head) and (D) multiple sphenoid sinus septations.

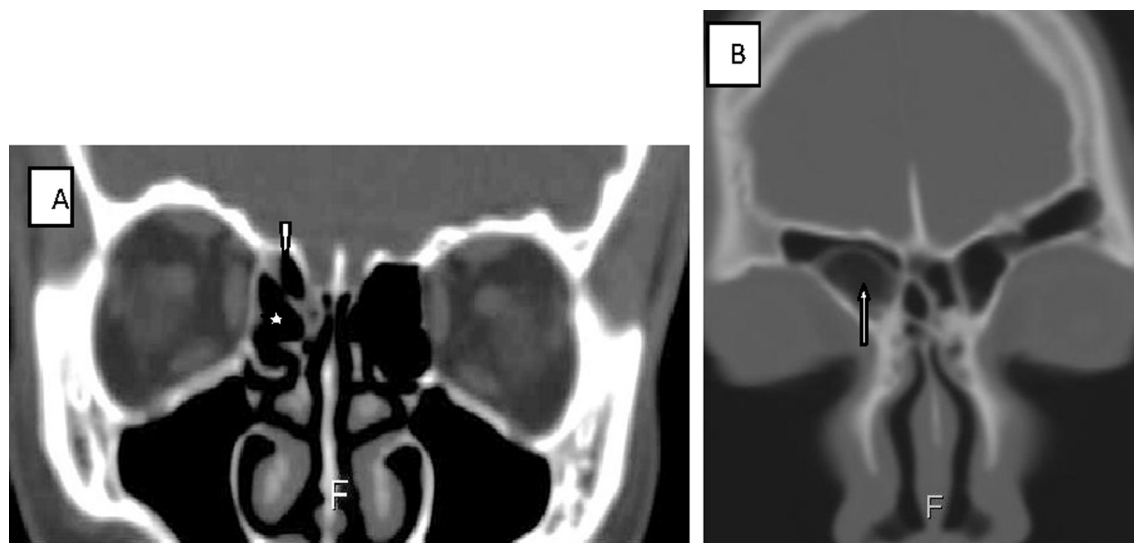


Fig. 8. Coronal CT images (A) frontal cell (arrow head), agger nasi cell (star), (B) type 4 Frontal cell (arrow).

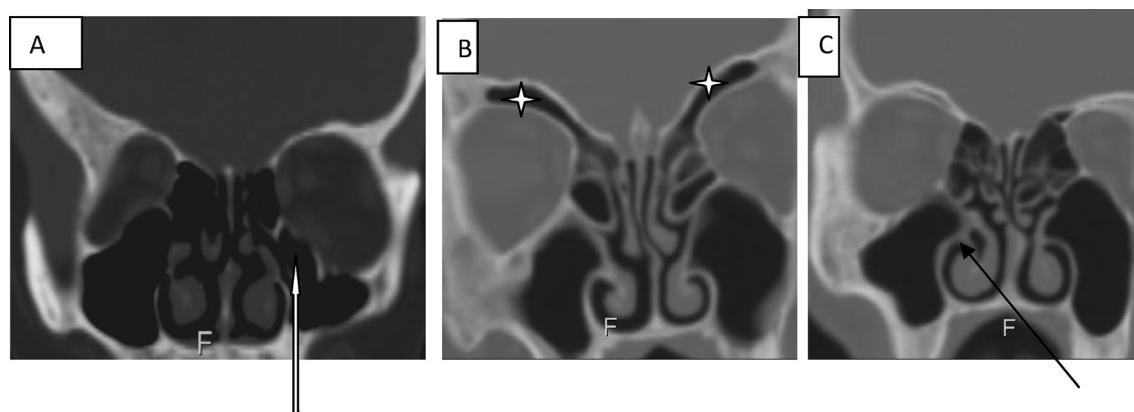


Fig. 9. Coronal CT images; (A) Haller's cell (white arrow), (B) supra-orbital cell (↔) and (C) pneumatization of right inferior turbinate (black arrow).

4.5. Ethmoidal sinus variation

Agger nasi cells (Fig. 8A): just anterior to the anterosuperior attachment of the middle turbinate and anterior to the frontal recess is the agger (ridge) nasi. The agger nasi cells are extramural cells and represent the most anterior ethmoid cells. The cells open into the ethmoidal infundibulum. They are the most common air cells that are not completely removed during functional endoscopic sinus surgery. This is because of its location hence allowing persistent mucosal disease and recurrent infection. The reported prevalence of this variant by various authors differs, Aramani et al.¹⁰ and Liu et al.²⁰ had very low prevalence of 1.9%, while Bolger et al.¹³ had very high prevalence of 98.5%. In this study we got a prevalence of 26% which is comparable to that of Dua et al.²¹ and Rashid et al.²² who got prevalences of 40% and 49% respectively.

Haller's cells (Fig. 8B): Progression of the ethmoid pneumatization process into an infraorbital location lead to formation of Haller's cells which are located below the ethmoid bulla, along the maxillary sinus roof and most inferior portion of the lamina papyracea. Haller cells can be clinically significant because of their strategic location along the course of the infundibulum. Such factors as the size of these air cells, their proximity to the natural ostia of the maxillary sinus, and evidence of inflammation within the cell may cause obstruction of the maxillary ostium and predispose to infections. Davis et al.,²³ associated Haller's cell to maxillary

chronic sinusitis. The prevalence of Haller's cells in this study was 20.91%. Similar findings were observed by Asruddin et al. 28%,⁷ Perez-pinas et al. 20%¹¹ and Dua et al. 16%.²¹ Aramani et al.¹⁰ and Liu et al.²⁰ recorded lower prevalence of 1.9% and 1% respectively.

Onodi cells (Fig. 7A) are most posterior ethmoid cells that migrated to the anterior region of the sphenoid sinus with antero-superior location and intimately related to the optic nerve. Disease conditions within these cells may cause optic neuropathy. Its proximity to the optic nerve is also of clinical importance as the nerve may be predispose to injury during ESS. The prevalence of onodi cells in this study was 7.27% which is similar to the prevalence recorded by Rashid et al.²² on cadaveric studies. Higher prevalences ranging from 39% to 60% had been recorded.^{24,25}

Supraorbital cells (Fig. 9B): Supraorbital ethmoid cells are the ethmoid cells that extend superolaterally between the middle orbital wall and the ethmoid roof. Supraorbital ethmoid cells may simulate multiple frontal sinuses on coronal CT images. According to Zhang et al.,²⁶ it has a prevalence of 5.4%.

Frontal cells or Kuhn's cells (Fig. 8A and B): These are ethmoid cells intimately related to agger nasi cells. They are classified into four different types according to their pneumatization. We observed frontal cells in 8.73% of the 110 patients studied. Park et al.²⁷ found frontal cells in 32% of the 105 patients in their study.

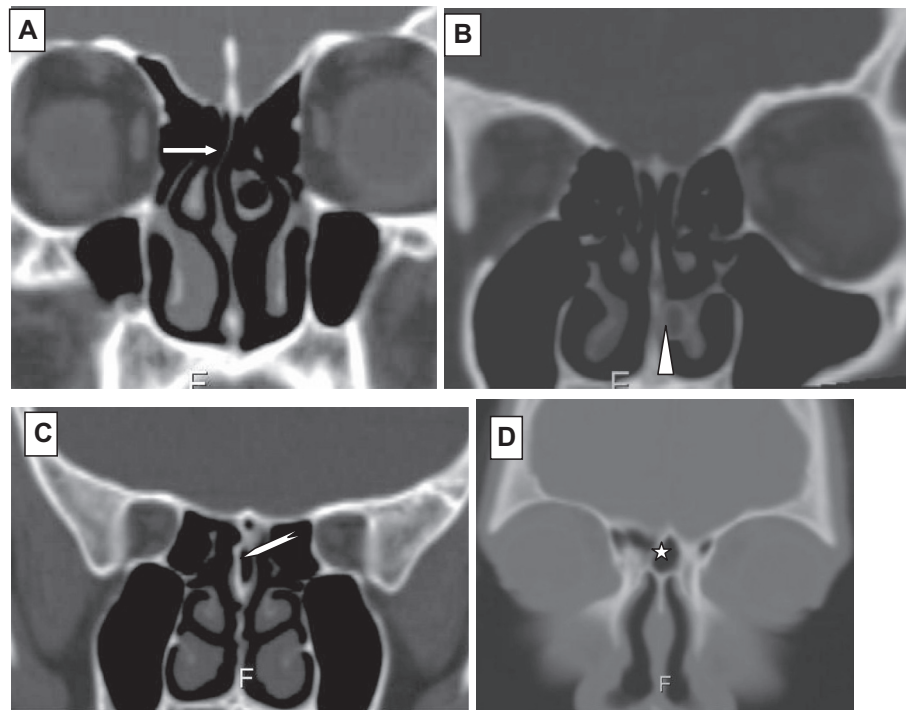


Fig. 10. Coronal CT images showing (A) nasal septum deviation (arrow), (B) nasal septum spur fused with left inferior turbinate (arrow head), (C) pneumatisation of nasal septum (chevron) and (D) pneumatisation of crista galli.

4.6. Nasal septum variation

Variation in the nasal septum results in morphological variations such as nasal septal deviation (NSD) (Figs. 4A and 10A), chondrovomer junction deformity, pneumatisation of nasal septum (Fig. 10C) and nasal bone spur. Septal deviation is a shift in the midline position of the septum to either left or right, and may be cartilaginous, osseous or combined deviation involving the osseous or cartilaginous part of the septum. It may be associated with deformity or asymmetry of the adjacent turbinate or with nasal wall structures. The prevalence is variable in the population. Nasal septal spur (Fig. 10B) is a generally asymptomatic bone deformity that may cause restriction of the nasal air flow. There could also be fusion of the turbinate with nasal septum (Fig. 10B). In our study we observed septal deviation in 20.91% of our participants. There was only one case of septal spur with fusion to the left nasal turbinate. Some studies have recorded different prevalence of NSD which ranged from 14.1 to 80%. Dutra and Marchiori²⁸ recorded 14.1%, Dua et al.²¹, and Asruddin et al.⁷ found prevalence of 44% and 38% in their study respectively. Higher prevalence were found in studies by Mamitha et al.⁸, and Aramani et al.¹⁰ who got 65% and 74.1% respectively.

5. Conclusion

The findings in this study shows that anatomical variations in the paranasal sinuses and nasal cavity are common. Computed tomography is the gold standard in the radiologic investigation of the paranasal sinuses, either for diagnosis of the sinonasal lesions or pre and post -surgical assessment. Its capability in delineating the anatomical variants in paranasal sinuses protects against iatrogenic injury to essential structures around the paranasal sinuses and recurrent diseases from extramural cells. It is of paramount importance that computed tomography of the paranasal sinuses in three dimensions of axial, coronal and sagittal imag-

ing be acquired and adequately reviewed prior to functional endoscopic sinus surgery (FESS).

References

1. Vivek G, Khandelwal N. Imaging of paranasal sinuses. In: Niranjana K, Veena C, Arun KG, editors. *Diagnostic radiology: neuroradiology including head and neck imaging*. Jaypee Brothers Medical Publishers(P) LTD; 2010:366–86.
2. Zinreich SJ, Albayram S, Benson ML, Oliverio PJ. The osteomeatal complex and functional endoscopic surgery. In: Som PM, Curtin HD, editors. *Head and neck surgery*. St Louis: Mosby Inc.; 2003:149–73.
3. Anthony JS, Harnsberger HR, Richard SB. Pneumatization of the paranasal sinuses: normal features of importance to the accurate interpretation of CT scans and MR images. *AJR*. 1993;160:1101–1104.
4. Teatini G, Simonetti G, Salvolini U, et al. Computed tomography of the ethmoid labyrinth and adjacent structures. *Ann Otol Rhinol Laryngol*. 1987;96:239–250.
5. Kasper KA. Nasofrontal connections. A study based on one hundred consecutive dissections. *Arch Otolaryngol*. 1936;23:322–344.
6. Miranda CMNR, Maranhao CPM, Arraes FMNR, et al. Anatomical variations of paranasal sinuses at multislice computed tomography: what to look for. *Radiol Bras*. 2011;44:256–262.
7. Asruddin, Yadav SPS, Yadav RK, Singh J. Low dose CT in chronic sinusitis. *Indian J Otolaryngol*. 1999–2000;52:17–22.
8. Mamitha H, Shamasunder NM, Bharathi MB, Prasanna LC. Variations of osteomeatal complex and its applied anatomy: a CT scan study. *Indian J Sci Technol*. 2010;3:904–907.
9. Weinberger DG, Anand VK, Al-Rawi M, Cheng HI, Messina AV. Surgical anatomy and variations of the onodi cell. *Am J Rhinol*. 1996;10:365–370.
10. Aramani A, Karadi RN, Kumar S. Anatomical variation in osteomeatal complex. *J Clin Diagn Res*. 2014;8:01–04.
11. Perez-Pinas I, Sabate J, Carmona A, Catalina Herrera CJ, Jimenez-Castellanos J. Anatomical variations in the human paranasal sinus region studied by CT. *J Anat*. 2000;197:221–227.
12. Scribano E, Ascenti G, Casio F, Racchiusa S, Salamone I. Computerized tomography in the evaluation of anatomic variations of the osteomeatal complex. *Radio Med (Torino)*. 1993;86:195–199.
13. Bolger WE, Butzin CA, Parsons DS. Paranasal sinus bony anatomic variations and mucosal abnormalities: CT analysis for endoscopic sinus surgery. *Laryngoscope*. 1991;101:56–64.
14. Delano MC, Fun FY, Zinrich SJ. Relationship of the optic nerve to the posterior paranasal sinuses: a CT anatomic study. *Am J Neuroradiol*. 1996;17:669–675.
15. Liu S, Wang Z, Zhou B. Related structures of the lateral sphenoid wall anatomy studies in CT and MRI. *Lin Chuang Er Bi Yan Hou Ke Za Zhi*. 2002;16:407–409.

16. Basic N, Basic V, Jukic T, et al. Computed tomographic imaging to determine the frequency of anatomical variations in pneumatization of the ethmoid bone. *Eur Arch Otorhinolaryngol*. 1999;256:69–71.
17. Som PM, Park EE, Naidich TP, Lawson W. Crista galli pneumatization is an extension of the adjacent frontal sinuses. *AJNR Am J Neuroradiol*. 2009;30:31–33.
18. Mohammad HD, Daryani Amir. Evaluation of anatomic variants of paranasal sinuses. *Internet J Otorhinolaryngol*. 2007;1:1–5.
19. Stallman JS, Lobo JN, Som PM. The incidence of concha bullosa and its relationship to nasal septal deviation and paranasal sinus disease. *AJNR Am J Neuroradiol*. 2004;25:1613–1618.
20. Liu X, Zhan G, Xu G. Anatomical variations of osteomeatal complex and correlation with chronic sinusitis: CT evaluation. *Zhonghua Er Bi yan Hou Ke Za Zhi*. 1999;34:143–146.
21. Dua K, Chopra H, Khurana AS, Munjal M. CT scan variations in chronic sinusitis. *Indian J Radiol Image*. 2005;15:315–320.
22. Rashid A, Deep B, Wameedh A, Yahya A, Sukhpal S. Clinically significant anatomical variants of the paranasal sinuses. *Oman Med J*. 2014;29:110–113.
23. Davis WE, Templer J, Parsons DS. Anatomy of the paranasal sinuses. *Otolaryngol Clin North Am*. 1996;29:57–91.
24. Driben JS, Bolger WE, Robles HA, et al. The re-liability of computerized tomographic detection of the Onodi (sphenothmoid) cell. *Am J Rhinol*. 1998;12:24.
25. Thanaviratananich S, Chaisiwamongkol K, Kraitrakul S, et al. The prevalence of an Onodi cell in adult Thai cadavers. *Ear Nose Throat J*. 2003;82:200–204.
26. Zhang L, Han D, Ge W, et al. Computed tomographic and endoscopic analysis of supraorbital ethmoid cells. *Otolaryngol Head Neck Surg*. 2007;137:562–568.
27. Park SS, Yoon BN, Cho KS, et al. Pneumatization pattern of the frontal recess: relationship of the anterior-to-posterior length of frontal isthmus and/or frontal recess with the volume of agger nasi cell. *Clin Exp Otorhinolaryngol*. 2010;3:76–83.
28. Dutra DL, Marchiori E. Helical CT of the paranasal sinuses in children; evaluation of inflammatory sinus disease. *Radiol Bras*. 2002;35:161–169.